Available online at www.sciencedirect.com
ScienceDirect
Applied Thermal Engineering 28 (2008) 1925–1931
APPLIED THERMAL ENGINEERING
www.elsevier.com/locate/apthermeng

3-D Numerical analysis on heating process of loads within vacuum heat treatment furnace

Xiaowei Hao *, Jianfeng Gu, Nailu Chen, Weimin Zhang, Xunwei Zuo

School of Materials Science and Engineering, Shanghai Key Laboratory of Materials Laser Processing and Modification, Shanghai Jiao Tong University, Shanghai 200240, China

Received 6 December 2006; accepted 6 December 2007
Available online 22 January 2008

Abstract

A 3-D numerical heat transfer model integrated with an intelligent PID temperature control subroutine has been developed and employed in the computational simulation of the heating process of typical load within vacuum heat treatment furnace. The transient temperature field within the load was obtained and the relationship among thermal hysteresis time, maximal temperature difference, heating temperature and heating rate was analyzed in detail. The results indicate that the maximal temperature difference within the load, as well as the thermal hysteresis time, decreases with preheating temperature, and increases with heating rate. A set of qualitative relationship guiding the design of thermal schedule for vacuum heat treatment was proposed and thus an optimum heating process was achieved, which could not only reduce the heating time considerably, but also save energy effectively. The simulated heating curves on certain points fitted well with experimental ones, which validated the numerical model used in this study.

Keywords: Temperature field; Heat transfer; Numerical analysis; Thermal hysteresis time; Vacuum heat treatment

1. Introduction

Heating up process is one of the most important phases in the vacuum heat treatment process in terms of ultimate microstructure and properties of the loads under the treatment. During this heating process, a lot of energy will be consumed [1]. Thus, optimizing heating up process is of great significance to energy-saving and quality control. Since heating up in the vacuum furnace is dominantly affected by radiation, and vacuum furnace has the small thermal capacity, the temperature of the loads rises much slower than that of the furnace. This phenomenon is called thermal hysteresis [2–4]. Hence, it is necessary to consider the thermal hysteresis time during vacuum heating process. On principle the total heating time t of the batch-type vacuum heat treatment furnace consists of three sequential parts t_a, t_b, t_c [3,5,6]. The first part t_a is the time period during which the furnace temperature increases from room temperature to the set temperature; the following second part t_b is the time period during which the temperature of whole load uniformly reaches the preset temperature, namely the thermal hysteresis time; the third part t_c is the time period during which the original microstructure of load transforms into austenite, usually the homogenizing time of austenite is also included. In general, t_c is solely dependent on the material type of loads while t_a and t_b are mainly related to heating temperature, heating rate, the shape and size of the loads as well as whether preheating is performed or not. Therefore, determining t_a and t_b accurately becomes the key to the optimization of vacuum thermal schedule.

In the past, extensive experimental researches on thermal schedule of vacuum heat treatment have been made, which came out with various empirical formulae [3,5,7,8]. These empirical models, however, show a rather large deviation from the actual processes. So far, there is still no general rule to follow in designing optimal thermal schedule.

* Corresponding author. Tel.: +86 2134203743; fax: +86 2134203742.
E-mail address: haoxw@sjtu.edu.cn (X. Hao).

1359-4311/$ - see front matter © 2007 Elsevier Ltd. All rights reserved.
doi:10.1016/j.applthermaleng.2007.12.007

Nomenclature

a	absorption coefficient (m^{-1})
E	energy (J)
h	species enthalpy ($J\ kg^{-1}$)
I	radiation intensity ($W\ m^{-2}\ sr^{-1}$)
I_0	boundary intensity for $\vec{s}$ ($W\ m^{-2}\ sr^{-1}$)
$\vec{J}$	diffusion flux vector ($kg\ m^{-2}\ s^{-1}$)
n	refractive index
p	pressure (Pa)
$\vec{r}$	position vector
s	path length (m)
$\vec{s}$	direction vector
$\vec{s}'$	scattering direction vector
S_h	volumetric heat source ($W\ m^{-3}$)
t	time (s)
T	temperature (K)
q	heat flux ($W\ m^{-2}$)
V_h	volume of heating rods (m^3)
P_f	power of furnace (W)
k	thermal conductivity ($W\ m^{-1}\ K^{-1}$)

Greek symbols

α	controlling heating coefficient
ε	emissivity
Φ	phase function
$\vec{v}$	velocity vector ($m\ s^{-1}$)
ρ	density ($kg\ m^{-3}$)
σ	Stefan–Boltzmann constant, 5.671×10^{-8} ($W\ m^{-2}\ K^{-4}$)
σ_s	scattering coefficient (m^{-1})
$\bar{\bar{\tau}}$	stress tensor (Pa)
Ω'	solid angle (sr)

Subscripts

eff	effective
in	incidence
j	species
out	leaving the surface
PID	proportional, integral, derivative
w	wall

Moreover, the above experimental methods have many disadvantages such as high cost, long cycle, and less applicable for complicated loads or furnaces [4,9]. Recently, computational simulation technology has been widely used in the simulation of heating processes of steel loads in continuous industrial annealing furnace, fluidized bed furnace, tempering furnace, pusher-type furnace and other reheating furnaces [9–16]. Monte Carlo method, FDM and FEM have been used by Mochida [17], Kang [18] and Wang [4], respectively in numerical simulation on heat transfer process in vacuum heat treatment furnace. However, the above-mentioned models have their obvious limitation, some apply for two-dimensional simple-shaped loads, and some neglect temperature gradient in the furnace and loads. At the same time little attention is paid on simulation of controlled heating process of furnace. The typical temperature control method in the vacuum furnace is PID controller (where PID represents proportional, integral, and derivative). When the measured temperature is deviates from the set temperature, the heating input is regulated to minimize the deviation. It is a typical feedback control system.

Taking the vacuum furnace and loads as a whole system, a 3-D numerical model was established in this paper. In order to simulate the actual temperature control of the furnace, an intelligent PID subroutine was especially developed and integrated in the model. Transient heat transfer of typical loads during heating process and the thermal hysteresis phenomenon were closely investigated. The transient temperature gradient distribution in the loads was successfully predicted, and an optimized thermal schedule was proposed based on multiple simulations.

2. Mathematical model of heat transfer

The models of heat transfer in vacuum heat treatment furnace include conduction, radiation and convection. The convection may be neglected since there is almost no atmosphere in vacuum environment during heating process. Heat transfer models used in this simulation can be described as follows:

Energy equation:

$$\frac{\partial}{\partial t}(\rho E) + \nabla \cdot (\vec{v}(\rho E + p)) = \nabla \cdot \left(k_{\text{eff}} \nabla T - \sum_j h_j \vec{J}_j + (\bar{\bar{\tau}}_{\text{eff}} \cdot \vec{v}) \right) + S_h \quad (1)$$

In solid regions, energy transport equation can be simplified as

$$\frac{\partial}{\partial t}(\rho h) = \nabla \cdot (k \nabla T) + S_h \quad (2)$$

Volumetric heat source (S_h) of heating rods can be determined by

$$S_h = \alpha_{\text{PID}} \cdot P_f / V_h \quad (3)$$

where α_{PID} is a coefficient which is presented by the intelligent PID temperature control subroutine.

Radiation model:

Radiative heat transfer within vacuum furnace is calculated by DO (discrete-ordinates) radiation model. The DO radiation model solves the radiative transfer equation (RTE) for a finite number of discrete solid angles, each associated with a vector direction $\vec{s}$ fixed in the global Cartesian system (x, y, z). It transforms RTE into a transport equation for radiation intensity in the spatial

coordinates (x, y, z) and solves for as many transport equations as there are directions $\vec{s}$. The RTE goes as follows:

$$\frac{\mathrm{d}I(\vec{r},\vec{s})}{\mathrm{d}s} + (a+\sigma_s)I(\vec{r},\vec{s}) = an^2\frac{\sigma T^4}{\pi} + \frac{\sigma_s}{4\pi} \times \int_0^{4\pi} I(\vec{r},\vec{s}')\Phi(\vec{s},\vec{s}')\mathrm{d}\Omega' \quad (4)$$

Boundary and initial conditions:

Solid walls in vacuum furnace are assumed as gray walls whose boundary conditions can be specified as incidence radiation heat flux in the wall q_{in} and net radiation heat flux away from the wall q_{out}, respectively. Here

$$q_{in} = \int_{\vec{s}\cdot\vec{n}>0} I_{in}\vec{s}\cdot\vec{n}\,\mathrm{d}\Omega \quad (5)$$

$$q_{out} = (1-\varepsilon_w)q_{in} + n^2\varepsilon_w\sigma T_w^4 \quad (6)$$

For all the directions away from the wall $\vec{s}$, radiation intensity of the wall is $I_0 = \frac{q_{out}}{\pi}$. During the whole heating process, the temperature at the water-cooled walls is considered to be a constant. The temperature at other regions of the furnace and in the load is set to 20 °C as the initial condition.

3. Simulation of vacuum heating process

The vacuum heat treatment furnace and the load used in this work are a high pressure gas quenching furnace model VHQ-446HF and a die block of H13 steel respectively. Schematic structure of the vacuum furnace is presented in Fig. 1a. Dimensions of the working zone is 400 × 400 × 600 (mm) and the highest heating temperature is 1320 °C. The heating chamber of the furnace consists of furnace vessel with a water-cooled jacket, heaters made from graphite tubes, controlling thermocouple and thermal insulation walls. Twelve heating rods disperse uniformly along the circumferential direction in the heating chamber and the controlling thermocouple is located near the working zone. The load block with the size of 230 × 250 × 370 (mm) was placed at the center of the working zone. Some holes were drilled into the block for positioning surface and core work thermocouples (point T1 located on corner of the block, point T2 located on the center of the side surface and point T3 located body center of the block). These holes were 4 mm in diameter and 5 mm in depth (T1 and T2) or 115 mm in depth (T3).The specific positions of the monitoring thermocouples are shown in Fig. 1b.

The finite volume numerical model of the furnace was created based on a commercial code Fluent 6.1. Grid for the furnace and load is shown in Fig. 2. The furnace and load were modeled as a whole system. By applying symmetry plane, only a quarter of the structure needed to be modeled. After the 3-D CAD model of the furnace with controlling thermocouple was created, its numerical grid model was represented with a total of 410,000 tetrahedral cells.

Three-stage-heating schedule with preheating steps was employed based on early experiences (shown in Fig. 3). Preheating process, during which the heating process is carried out with different soaking stages, is usually designed to reduce the temperature difference within the load, and thus to minimize thermal distortion and crack. In initial schedule, the first preheating stage was set at 600 °C, the second preheating stage was set at 870 °C, and the heating temperature for last austenitizing stage was set at 1050 °C. The furnace was heated up to 600 °C at a low ramp rate of 5 °C/min and held at this preheating temperature for 180 min. Then it was heated up to 870 °C at the same rate of 5 °C/min and held for 120 min. And finally the ramp rate was reduced to 3 °C/min from 870 °C to austenitizing temperature 1050 °C and held for 120 min. The total heating stages took some 12 h. During heating process, the furnace temperature was controlled by PID temperature-control device, meanwhile the heating curves at the specific points in the load were measured with help of thermocouples.

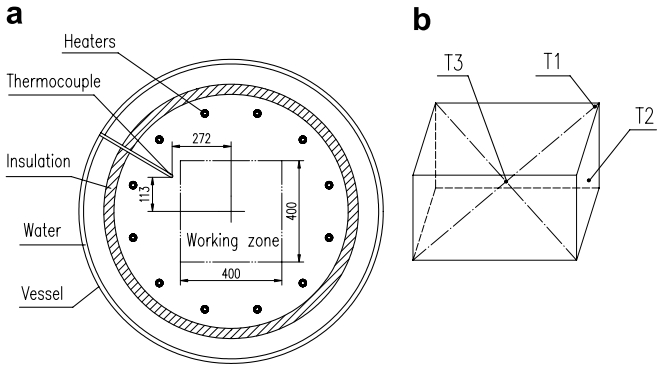

Fig. 1. Schematic of (a) the vacuum furnace and (b) the die block.

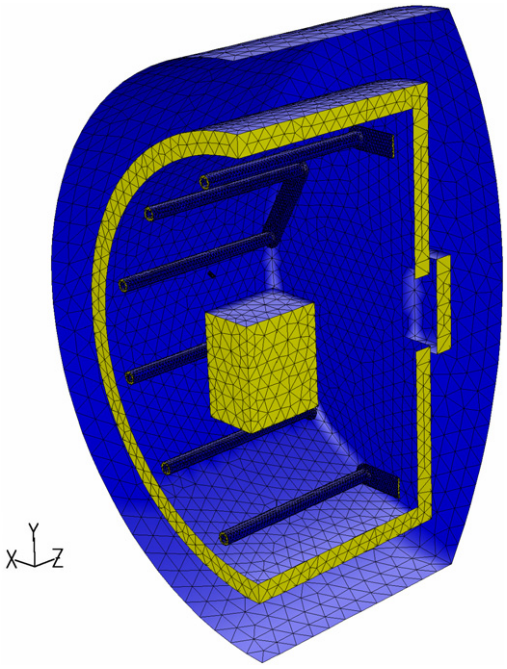

Fig. 2. Computational grid of the vacuum furnace with die block.

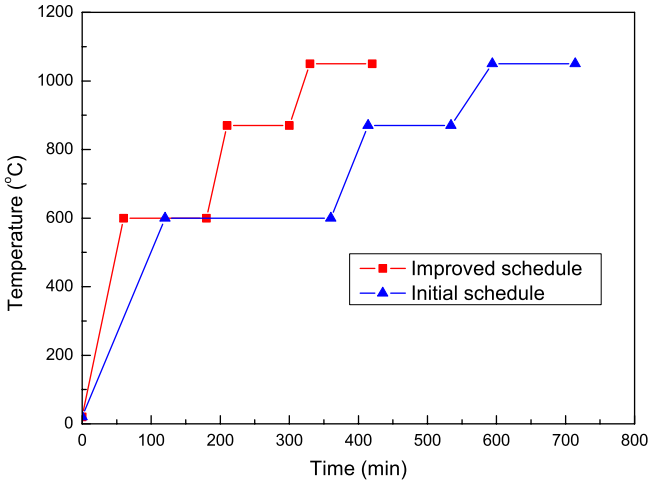

Fig. 3. Thermal schedules of the die block.

In order to accord with actual heating process and to obtain more accurate simulation results, an intelligent PID temperature control subroutine was developed with C through Fluent UDF (user defined function) interface. The calculating flow chart including PID subroutine is illustrated in Fig. 4. The program starts with user-defined initialization, and then the solution iteration loop begins with adjust of boundary conditions. Next, the energy equations are solved sequentially, followed by properties updates. The PID subroutine is called in each iteration loop. When the current temperature of controlling thermocouple (i.e. the furnace temperature) read by PID subroutine is different from the set furnace temperature, the control coefficient α_{PID} will be calculated, and then the source term S_h of heating rods will be adjusted according to Eq. (3) to minimize the error. Finally, a check for convergence and end time is performed, determining whether the loop continues or exits.

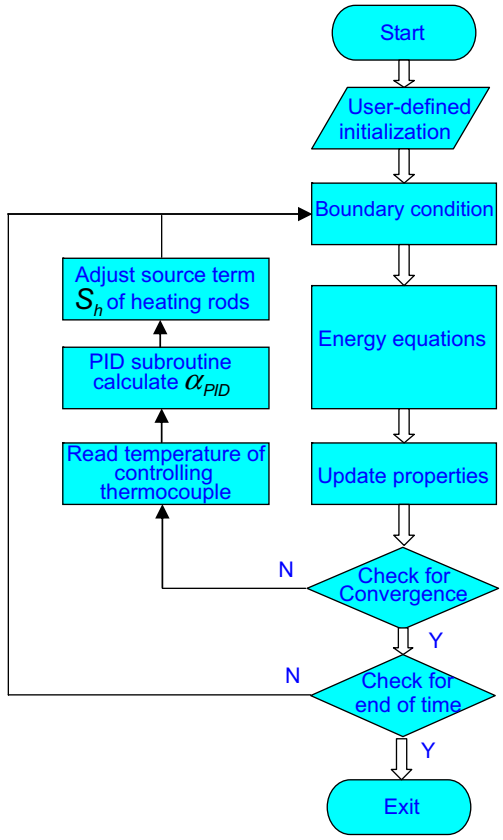

Fig. 4. Calculating flow chart with PID control subroutine.

4. Results and discussion

Simulated temperature contours of the furnace and the load at 120 min are presented in Fig. 5a and b, respectively. It can be seen that there exists large temperature gradient between the furnace and the load. At this time, the furnace temperature has reached the first preheating temperature 600 °C. However, it can be found that the temperature at T1 point, on which the heating rate is the fastest, is only around 379 °C. In the body center (T3 point) it is even lower at 258 °C. Therefore, the thermal hysteresis phenomenon is very evident. Fig. 6a shows the simulated heating curves for initial schedule, which indicates that the furnace temperature (TF) curve is well controlled. Hence, the user defined PID temperature control subroutine is successful for vacuum heat treatment simulation. The curves of the temperature difference with time are given in Fig. 6b, where the maximal temperature difference between furnace and load (TF–T3) as well as within the load (T1–T3) decreases with the heating temperature, indicating the less thermal hysteresis with higher heating temperature. In addition, it can also be found in Fig. 6a that the thermal hysteresis time at heating temperature of 600 °C, 870 °C and 1050 °C are 160 min (t_{b1}), 100 min (t_{b2}) and 60 min (t_{b3}), respectively. Therefore the thermal hysteresis time reduces with the heating temperature, i.e. $t_{b1} > t_{b2} > t_{b3}$. This is can be explained by the lower radiative heat transfer efficiency at lower temperature range, which results in the slow increase of load temperature. In principle, when the three-stage-heating schedule is designed, the holding time at each stage should conform to the relationship of $t_1 > t_2 > t_3 - t_c$.

Such relationships can also be found in Fig. 6a as $t_1 > t_{b1}$ and $t_2 > t_{b2}$, which tells that the holding time for the first and second stage is too long and exceeds the relevant thermal hysteresis time, leading to that load temperature at center has already reached preheating temperature long before the end of the first and second preheating stage. Whereas the goal of the preheating is to reduce the temperature difference between the load surface and center without reducing the temperature difference to zero. According to the thermal schedule recommended by North American Die Casting Association (NADCA) [19], next heating stage can be started as soon as the temperature difference between surface and center is less than 30 °C. In this sense, the holding time for the first and second preheating stage should be reduced accordingly so as to ensure

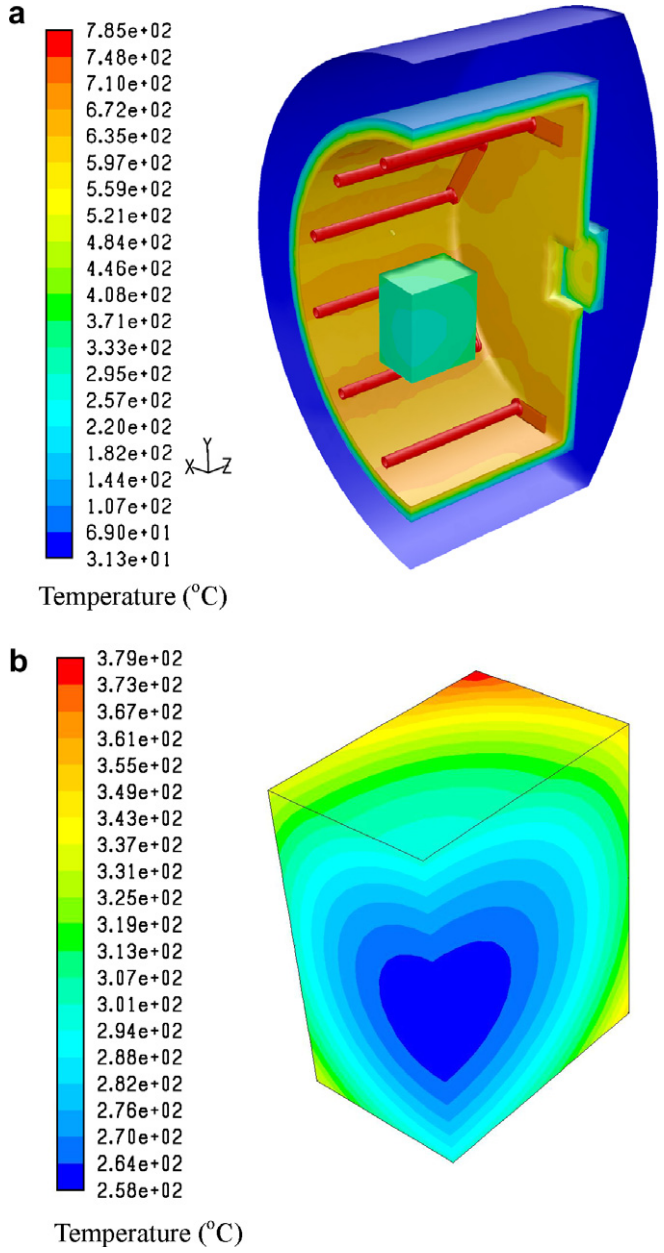

Fig. 5. Simulated temperature contours at 120 min for initial schedule (a) the furnace and (b) the load.

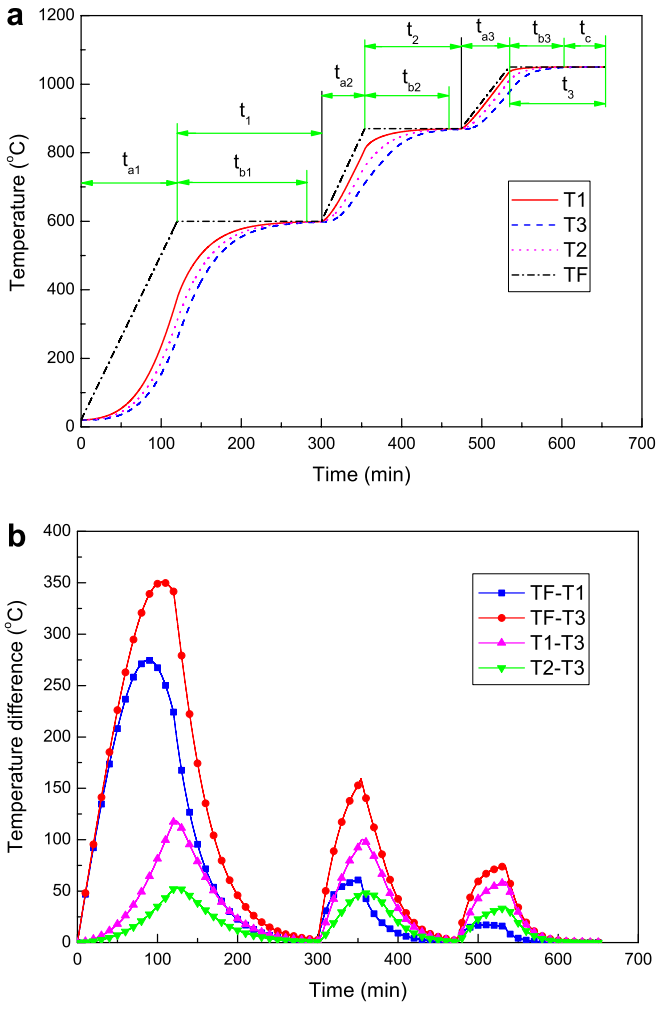

Fig. 6. Simulated results for initial schedule (a) heating curves and (b) temperature difference curves.

$t_1 < t_{b1}$ and $t_2 < t_{b2}$. Besides, the microstructure transformation time for H13 steel is about 30 min, so the holding time (t_3) for the third stage should be 90 min ($t_{b3} + 30$), while the current holding time for initial schedule is 120 min. Therefore t_3 should also be considerably reduced. It can also be seen in Fig. 6b that the maximal temperature difference between load surface and body center is less than 50 °C, thus, the time for heating up at each stage t_{a1}, t_{a2} and t_{a3} should be appropriately reduced in order to increase the heating rate of the furnace.

The initial thermal schedule need to be further improved due to the above-mentioned irrationality. An optimum schedule was obtained based on multiple simulations, which increased the heating rate at the first, second and third stage to10 °C/min, 9 °C/min and 6 °C/min, reduced the holding time of each stage to 2 h, 1.5 h and 1.5 h, respectively. The improved schedule can be found in Fig. 3.

The simulated heating up and temperature difference curves of the improved schedule are shown in Fig. 7a and b, respectively. Comparison between Figs. 6 and 7 tells that the maximal temperature difference between furnace and load as well as within the load increases with the heating rate, i.e. larger thermal hysteresis effect. The thermal hysteresis time t_{b3} at the third stage can be as long as 63 min, slightly longer than the initial schedule. However, the absolute value of maximal temperature difference on surface and at body center is less than 60 °C and the increasing amplitude, compared to the initial schedule, is as small as 10 °C or so. The temperature difference between the surface (T2) and body center (T3) at the end the first and second preheating stage is less than 20 °C and 15 °C respectively, in accordance with the requirement of the schedule recommended by NADCA, and thus there exists the possibility to decrease the holding time of preheating even further. At the third heating stage, another 27 min for microstructure transformation is left after the whole load reaches the austenitizing temperature. All in all, the

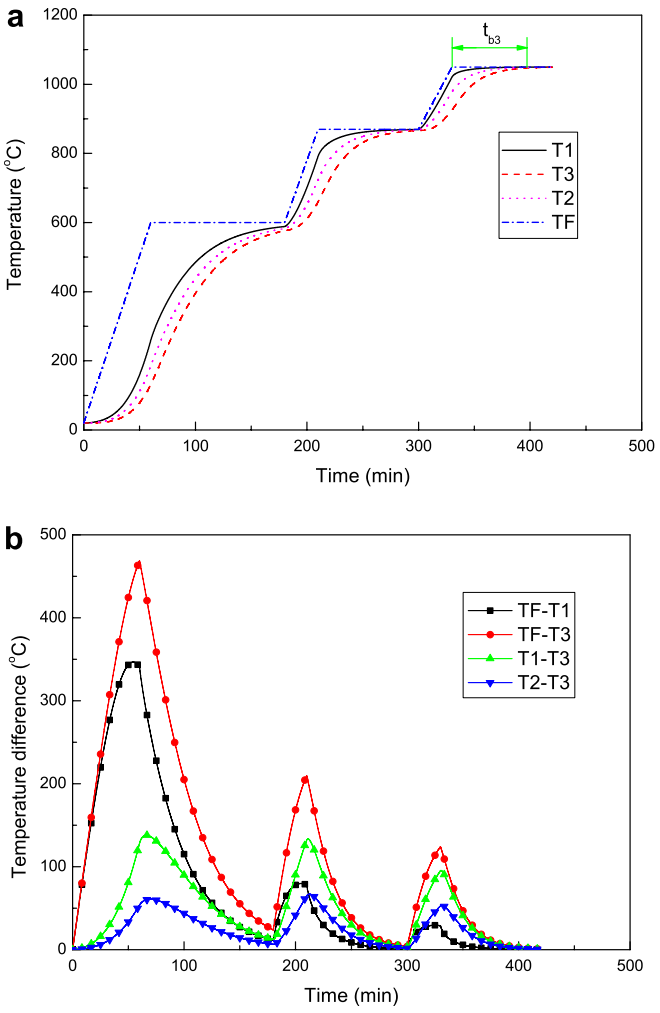

Fig. 7. Simulated results for improved schedule (a) heating curves and (b) temperature difference curves.

improved schedule not only meets the heating demand of the load, but also saves energy considerably. The total heating time is reduced by 5 h compared with the initial schedule.

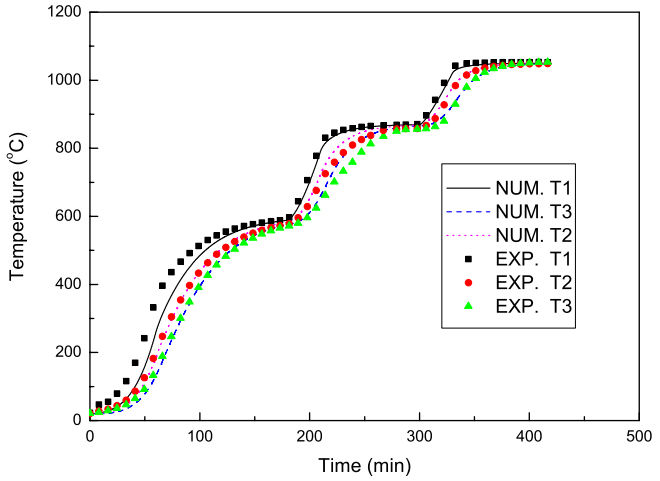

Fig. 8. Comparison of simulated and measured results.

The comparison between the simulated heating curves and experimental ones for the improved thermal schedule is shown in Fig. 8. It can be seen that the simulated curves at side surface (T2) and body center (T3) agree very well with the measurements except the period during which the load temperature is around 800 °C. The deviation in this period may be attributed to the phase transformation and linearization approximation of some properties. Similarly, the simulated heating curve at the load corner (T1) agree well with experimental result, and have a relatively lower temperature than the latter at lower temperature stage, which may be due to the unfavorable placement of the thermocouples or the error of temperature-measuring system.

5. Conclusions

In this study, taking load and vacuum furnace as a complete system, a 3-D transient heat transfer model was established, and a PID temperature control subroutine was developed in the model. The heating process of a block load was simulated based on the model. The results are concluded as following:

(1) The user defined PID subroutine was applied successfully for the furnace temperature control in the simulation of the actual heating process in vacuum furnace, which improved the simulating accuracy.
(2) The analysis of the simulation on heating process of block load revealed that the maximal temperature difference within load, as well as the thermal hysteresis time, decreased with preheating temperature and increased with heating rate.
(3) Some qualitative relationship guiding the design of vacuum heating schedules was put forward based on the simulation, and as a result, an improved thermal schedule was obtained which greatly shortened the heating time.
(4) The comparison between simulation results and experimental ones showed that the proposed numerical model could rather accurately predict the heating process in vacuum heat treatment furnace, and our simulation could provide important guidance for the design and improvement of vacuum thermal schedule.

Acknowledgement

This work is supported by Key Foundation Program of Shanghai Science & Technology Committee under Grant No. 06JC14036.

References

[1] J. Kang, T. Huang, R. Purushothaman, W. Wang, Y. Rong, Modeling and simulation of heat transfer in loaded continuous heat treatment furnace, Transactions of Materials and Heat Treatment 25 (2004) 764–768.

[2] C.P. Yan, Vacuum and Controlled Atmosphere Heat Treatment, Press of Chemical Industry, Beijing, 2006.
[3] S.Q. Zhang, Study on vacuum heat treatment thermal hysteresis time, Heat Treatment of Metals 25 (2000) 38–39.
[4] M.W. Wang, L.W. Zhang, G.D. Jiang, Numerical simulation of vacuum heat treatment thermal hysteresis time of GH4169 superalloy workpiece, Transactions of Materials and Heat Treatment 25 (2004) 772–775.
[5] E. Bao, H.Y. Ren, The selection on technical parameters of vacuum heat treatment, Heat Treatment of Metals Abroad 26 (2005) 41–42.
[6] Dipl.-lng. B. Zieger, H. Schulte, Vacuum-heat treatment of hot-work steel, in: Proceedings of the Fourth International Conference on Quenching and the Control of Distortion, Chinese Heat Treatment Society, CMES, Beijing, May, 2003, pp. 401–408.
[7] F. Dong, The determination on heating time of vacuum heat treatment, Machinist Metal Forming 9 (2001) 56.
[8] J.G. Zhang, P.W. Cong, Vacuum heat treatment of hot-work die steel H13, Heat Treatment of Metals 30 (2005) 77–80.
[9] L.A. Tagliafico, M. Senarega, A simulation code for batch heat treatments, International Journal of Thermal Science 43 (2004) 509–517.
[10] A. Jaklic, F. Vode, T. Kolenko, Online simulation model of the slab-reheating process in a pusher-type furnace, Applied Thermal Engineering 27 (2007) 1105–1114.
[11] J. Harish, P. Dutta, Heat transfer analysis of pusher type reheat furnace, Ironmaking and Steelmaking 32 (2005) 151–158.
[12] D.O. Marlow, Modelling direct-fired annealing furnaces for transient operations, Applied Mathematical Modelling 20 (1996) 34–40.
[13] S.H. Han, S.W. Baek, S.H. Kang, C.Y. Kim, Numerical analysis of heating characteristics of a slab in a bench scale reheating furnace, International Journal of Heat and Mass Transfer 50 (2007) 2019–2023.
[14] A. Jaklic, B. Glogovac, T. Kolenko, B. Zupancic, B. Teazk, A simulation of heat transfer during billet transport, Applied Thermal Engineering 22 (2002) 873–883.
[15] W.M. Gao, L.X. Kong, P.D. Hodgson, Numerical simulation of heat and mass transfer in fluidized bed heat treatment furnaces, Journal of Materials Processing Technology 125–126 (2002) 170–178.
[16] K.T. Januszkiewicz, Numerical model of the heating-up system with heating rods, Advances in Engineering Software 30 (1999) 141–145.
[17] A. Mochida, K. Kudo, Y. Mizutani, M. Hattori, Y. Nakamura, Transient heat transfer analysis in vacuum furnaces heated by radiant tube burners, Energy Conversion and Management 38 (1997) 1169–1176.
[18] J. Kang, Y.K. Rong, W. Wang, Numerical simulation of heat transfer in loaded heat treatment furnaces, Journal De Physique IV 120 (2004) 545–553.
[19] North American Die Casting Association, NADCA recommended procedures for H13 tool steel, NADCA, Rosemont Illinois, 1997.